Progress In Electromagnetics Research C, Vol. 63, 131–142, 2016

An Experimental Study on the Effect of Commercial Triple Junction Solar Cells on Patch Antennas Integrated on Their Cover Glass

Taha Yekan* **and Reyhan Baktur**

Abstract—A patch antenna integrated on the cover glass of a commercial space-certified solar cell is examined. Test fixtures were fabricated to study the antenna designed at 4.9 GHz when there was an active solar cell under the antenna. It is found that the solar cell affects the input impedance of the antenna and causes a 2–3 dB gain reduction. Repetitive tests were performed to confirm that the effect from solar cells on the antenna remained the same regardless of the working states of the solar cell, type of cover glass, or the assembly of the solar panel.

1. INTRODUCTION

Integration of antennas with solar cells has important applications for small satellites [1], deep space exploration [2], and self-powered ground sensors [3]. Such an integration can be particularly valuable for a CubeSat (a very small satellite designed with modular components to have a minimum payload) [4] as the antennas, when effectively integrated with the solar cells, do not compete with solar cells for the limited surface real estate. There have been four main types of integrations reported: (1) antennas integrated under solar cells [1, 5–7]; (2) antennas integrated on the same plane with or on the side wall perpendicular to solar cells [8–10]; (3) antennas integrated on top of solar cells [11–18], and (4) parts of the solar cells function as antenna [19–21] (the antenna in [7] also belongs to this category as the solar cell above the antenna acts as a parasitic elements of the antenna). The third type of integration is of particular interest and promise to a CubeSat system as the antenna topology, especially when it is small or optically transparent, facilitates a possible modular design. Accordingly, it is important to understand the interaction between the solar cell and the antenna. The impact of the antenna on the solar cell can be estimated with relative ease. One may evaluate the shadow or blockage caused by the antenna on the solar cell to determine the reduction in the solar cell's efficiency. The experimental set-up for such a study is also straightforward. For the effect of the solar cell on the antenna integrated on top, the reported results are limited. The objective of the research in [14, 15] was on the transparency or bandwidth of the antenna, and hence, there is no report on the effect of the solar cell. The dielectric resonator antenna in [13] was reported to have little effect on the solar cell, however, there was not sufficient information given on the specific solar cell, and hence the conclusion from [13] may not be applicable to satellite solar cells. In addition, the form factor of the antenna may present pressure on the solar cells if they were to fly in space. A more comprehensive research by Shynu et al. [12] presented a solar cell model, simulated and measured antenna's parameters with and without solar cell. Because the study was performed on one single relatively large (larger than one side of a CubeSat) bare (i.e., without cover glass) solar cell, the results may not be applied to antennas integrated with other types of solar cells with different cover glass. In addition, commonly, the conductive layer of a solar cell is its electric positive plate [7]. Therefore, the designs where the integrated antenna uses the solar cell as ground may induce unknown compatibility issues.

Received 11 March 2016, Accepted 21 April 2016, Scheduled 28 April 2016
* Corresponding author: Taha Yekan (taha.shahvirdi@aggiemail.usu.edu).
The authors are with the Utah State University, USA.

Quantifying and presenting a reliable estimation of how commonly used CubeSat solar cells effect the antenna design not only impact communication link budget and payload, but also provide design guidelines for integrated solar cell antenna arrays. In addition, it is a common practice to bond solar cells with their cover glass using transparent adhesive. The effect of such adhesive has not been studied yet. The objective of this study is to provide a consistent assessment on the performance of the integrated antenna due to the solar cell beneath it while the two are electrically separated. This includes repetitive tests, experiments with different cover glass and solar panel assembly, and examining the antenna against different states of active solar cells.

2. METHOD

A commercial space solar cell always has a cover glass on top of the photovoltaic layer as protection. The existence of the cover glass is the design basis of the integrated patch antenna, where the cover glass acts as the dielectric substrate of the antenna.

2.1. Test Fixtures

To assess the effect of the solar cell on the antenna's performance, we prototyped a two-cell solar panel composed entirely of all space certified off-the-shelf components. The size and the material of the solar panel is compatible with a standard 1U CubeSat (i.e., it is a cube of 10 cm on each edge.). Two fixtures to study the effect of the solar cell on the antenna integrated on top, are shown in Fig. 1 and Fig. 2, where one fixture has a functional solar cell (Fig. 1) and the other one does not have (Fig. 2). The cross section view of the fixture with solar cell and antenna is illustrated in Fig. 3. From bottom to top, the layer information is as follows. The first layer is a copper plate that serves as the base of the solar panel and the ground for electronics. A thin Kapton sheet (orange colored sheet in Fig. 1) with a thickness of $t_k = 0.0508$ mm is placed on top of the ground, and then two triple-junction space-certified solar cells from EmCore [22], are connected together and mounted on top of the Kapton sheet. The Kapton sheet is to electrically isolate the bottom of the solar cell, which is a metal coating and is the electrical positive of solar cells, from the RF ground. The height of solar cells is $h_s = 0.15$ mm. On top of each solar cell is a AF32 cover glass [23], which is a standard space-certified material for solar cells in a deep space environment because of its very high optical transparency and high temperature tolerance. The height of the AF32 glass is $h = 1$ mm, the glass is pre-cut by the manufacture to cover the solar cell seamlessly. The dielectric constant (ϵ_r) and loss tangent ($tan\delta$) of the AF32 glass are 4.5 and 0.015, both being measured at X band [17]. Finally, a patch antenna is screen printed on the AF32 cover glass

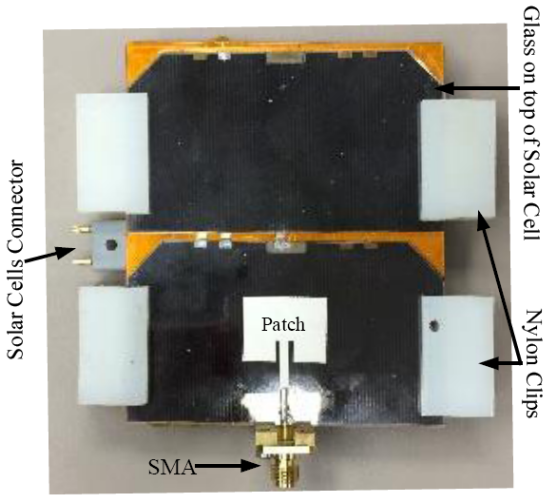

Figure 1. Patch antenna printed on AF32 cover glass with functional solar cells under it.

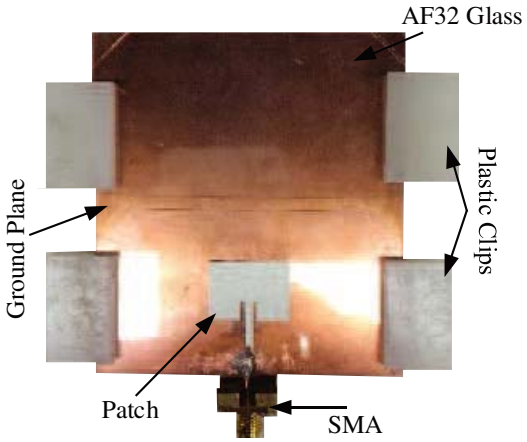

Figure 2. Patch antenna printed on AF32 glass without solar cells.

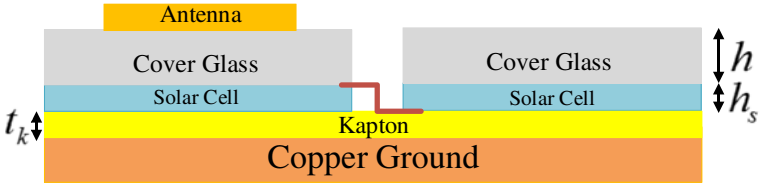

Figure 3. Cross section view of the fixture with solar cell and integrated antenna.

with silver based conductive ink (124-46 by Creative Material). It is obvious that the antenna uses the cover glass as its substrate, and the copper plate as the ground. It should be noted that, although there is only one solar cell with an antenna printed on its cover glass in the illustration (Fig. 3), the antenna integration is not limited to such a specific configuration. One may integrate antennas on each solar cell when needed.

For the fixture without solar cells (Fig. 2), the assembly is, from bottom to top, the copper plate, AF32 glass, and antenna. Because the Kapton sheet is very thin and casts negligible impact on the antenna's performance, we did not include the sheet in this fixture. One may include the sheet in the fixture without solar cells as long as it is carefully handled so that there are no air bubbles between the sheet and copper plate. In the fixture with solar cells (Fig. 1), the solar cells help to squeeze the air out. Both fixtures are then fastened on with four nylon clips machined in house.

2.2. Antenna Geometry

Figure 4 is an illustration of the geometry of the antenna integrated on a cover glass of the two-cell solar panel. The size of the solar panel, which is also the ground plane, is defined by W_G and L_G. The parameters L_S and L_C, together with W_G demonstrate the geometry of the cover glass, which is the same as the solar cells examined in this project. The spacing between the two solar cells can be easily determined from $L_G - 2L_S$. The design parameters for the patch antenna fed by a 50 Ω inset microstrip line are W, L, S_g, S_i, W_f and L_f. The antenna and microstrip line, operating at 4.9 GHz, were designed with Ansys' HFSS by considering the cover glass as the antenna's only substrate (i.e., the antenna integrated on the assembly shown in Fig. 2). The values of these design parameters are presented in Table 1. While printing the antenna on the cover glass with conductive ink, we repeated the printing process multiple times to ensure the thickness of the conductor is sufficiently higher than the microwave skin depth (i.e., 0.91 µm for the silver ink at 4.9 GHz).

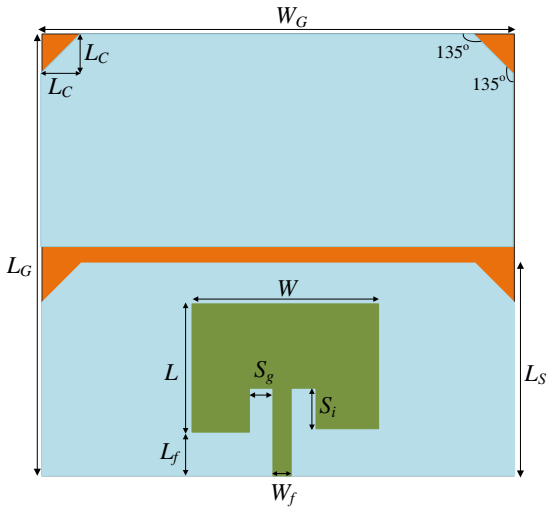

Figure 4. Geometry of the antenna integrated on a cover glass of the two-cell solar panel.

2.3. Measurement Setup

Performance of the antenna integrated on the AF32 glass with and without solar cells was examined using standard tests in an anechoic chamber. When the antenna is integrated on solar cells (Fig. 1), it is measured at different status of the solar panels such as without illumination or being illuminated by an artificial light. The two solar cells on the fixture in Fig. 1 were connected in series and have an output connector as shown. The connector not only allows us to measure the solar cells' output under illuminations, but also enables tests where we connect different resistive loads to the panel and then measure the antenna's performance.

Table 1. Geometrical parameters of the antenna on AF32 cover glass.

Parameter	Value (mm)	Parameter	Value (mm)
L_G	83	W	18
W_G	69	S_g	0.9
L_S	39.5	S_i	4.6
L_C	7.5	W_f	1.9
L	14	L_f	13.4

3. RESULTS AND DISCUSSIONS

3.1. Effect of the Solar Cell on the Microstrip Feed Line

As the patch antenna under study is excited using an inset feed microstrip line, it is important to first examine whether or not the solar cell affects the feed line. In order to do so, a 50 Ω microstrip line is designed and printed on a cover glass using the same assembly as the test fixture in Fig. 2. After being measured without solar cells (Fig. 5), the cover glass with printed microstrip line was measured on solar cell (Fig. 6), using the same assembly as in Fig. 1. The measured scattering parameters of the microstrip line are plotted in Fig. 7. From the measured S_{11} with and without solar cells, it is seen that the microstrip line is matched to the 50 Ω coax terminal at both cases, although matching is better when there is no solar cell. The S_{21} measurements indicate that there is loss when solar cell is present. This is understandable as the solar cell is a lossy substrate at RF frequency [12]. Overall, at the frequency of interest (4.9 GHz), the impedance of the microstrip line can be regarded as not being affected by the solar cell.

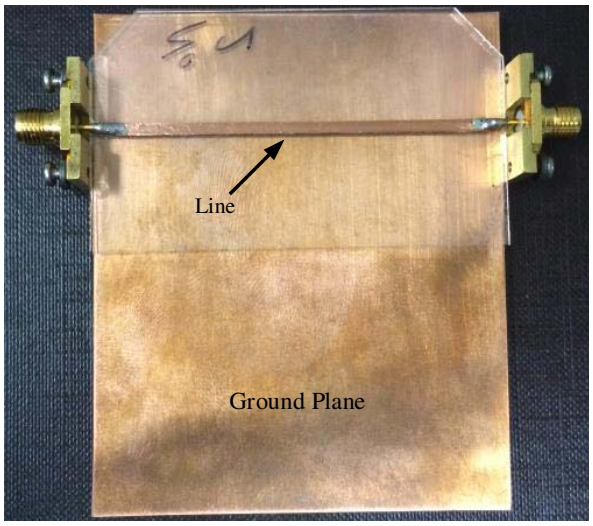

Figure 5. Examination of the microstrip feed line on AF32 glass.

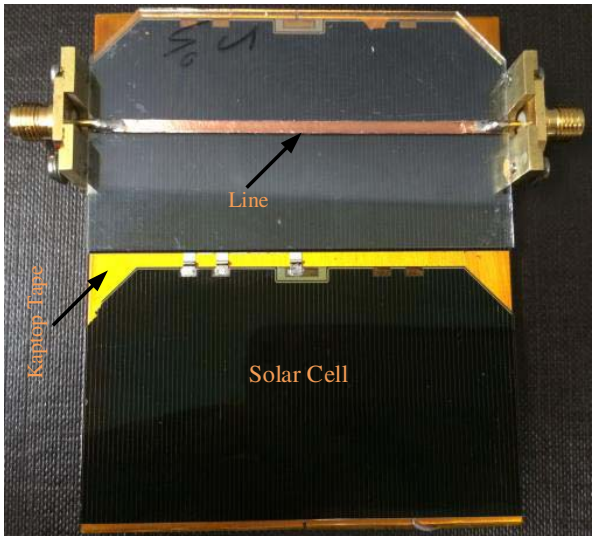

Figure 6. Examination of the microstrip feed line on AF32 glass with solar cells under it.

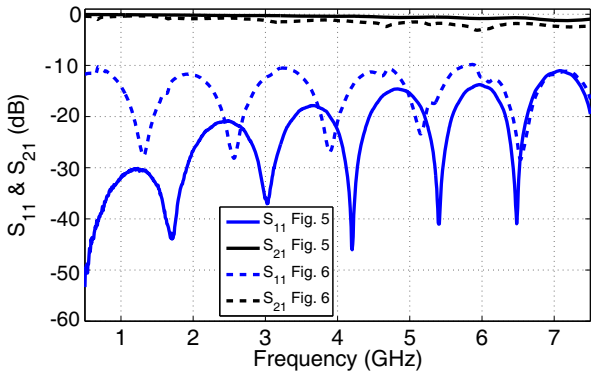

Figure 7. Measured scattering parameters of the microstrip feed line on AF32 glass with and without solar cells under it.

3.2. Effect of the Solar Cell on the Antenna

The antenna described in Section 2.2 was tested with and without solar cells using the fixtures in Fig. 1 and Fig. 2. The measured reflection coefficient is presented in Fig. 8. It is seen that the solar cell affected the input impedance of the antenna and its resonant frequency, shifting it from 4.89 GHz to 5.15 GHz. The reasons for the shift of frequency is studied in more detail in section 3.6, and the conclusion on the change of input impedance is obtained because of the test results on the feed line in section 3.1 where the impedance of the feed line was not affected by the solar cell. As a result, the antenna was tuned to achieve better impedance matching. The tuned antenna was then measured for its radiation pattern using a spherical scanner in an anechoic chamber. Fig. 9 presents the measured radiation pattern of the antenna with and without solar cells. Each radiation pattern is normalized to its co-polar maximum to see whether the solar cell affects the shape of the radiation pattern. It is seen that the shape and the cross-polar level of the antenna is not affected by the solar cells. The solar cell, as a lossy substrate beneath the cover glass for the antenna, has caused a decrease on the antenna's gain. In order to assess the gain loss of the antenna in a more reliable manner, we performed repetitive tests, where five identical antenna designs were printed on five AF32 cover glass with the same dimension and then the gain of these antennas were measured with and without the solar cells (the same two fixtures as described previously). The measured values of the antenna's gain are listed in Table 2. It is seen that, other than the No. 2 antenna, the gain difference between antenna with and without solar cells is consistent, and is somewhere between 2 and 3 dB. The data from the antenna No. 2 could be due to the printing procedure.

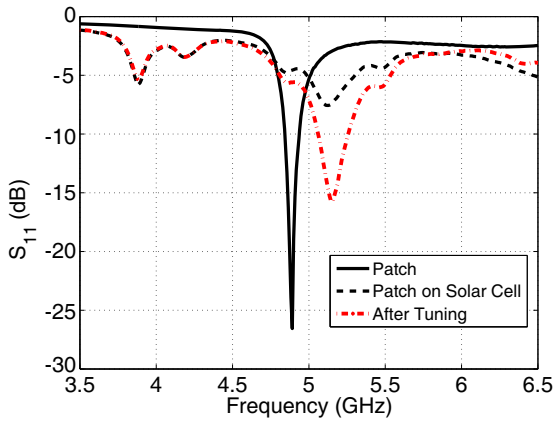

Figure 8. Effect of solar cells on the S_{11} parameter of the patch antenna.

Table 2. Repetetive tests: effect of the solar cell on the antenna's gain.

Antenna Number	1	2	3	4	5
Patch w/o Solar Cell Gain (dB)	6.1	4.9	6.5	5.84	6.1
Patch with Solar Cell Gain (dB)	3.12	3.32	3.37	3.37	3.32
Gain Difference (dB)	2.98	1.58	3.1	2.47	2.78

3.3. Repetitive Tests on Plexiglass as the Cover Glass

The examinations presented in the previous two sections were repeated by replacing the AF32 with off-the-shelf Plexiglass ($\epsilon_r = 2.6$, $\tan\delta = 0.0057$ at 1 MHz) that is easy to handle. This test is to ensure that the results from the previous two studies are not specific to a certain cover glass material. We kept the text fixtures the same as ones in Fig. 1 and Fig. 2, but changed the cover glass to Plexiglass. Accordingly we modified the antenna geometry and the feed line. The geometrical and design parameters

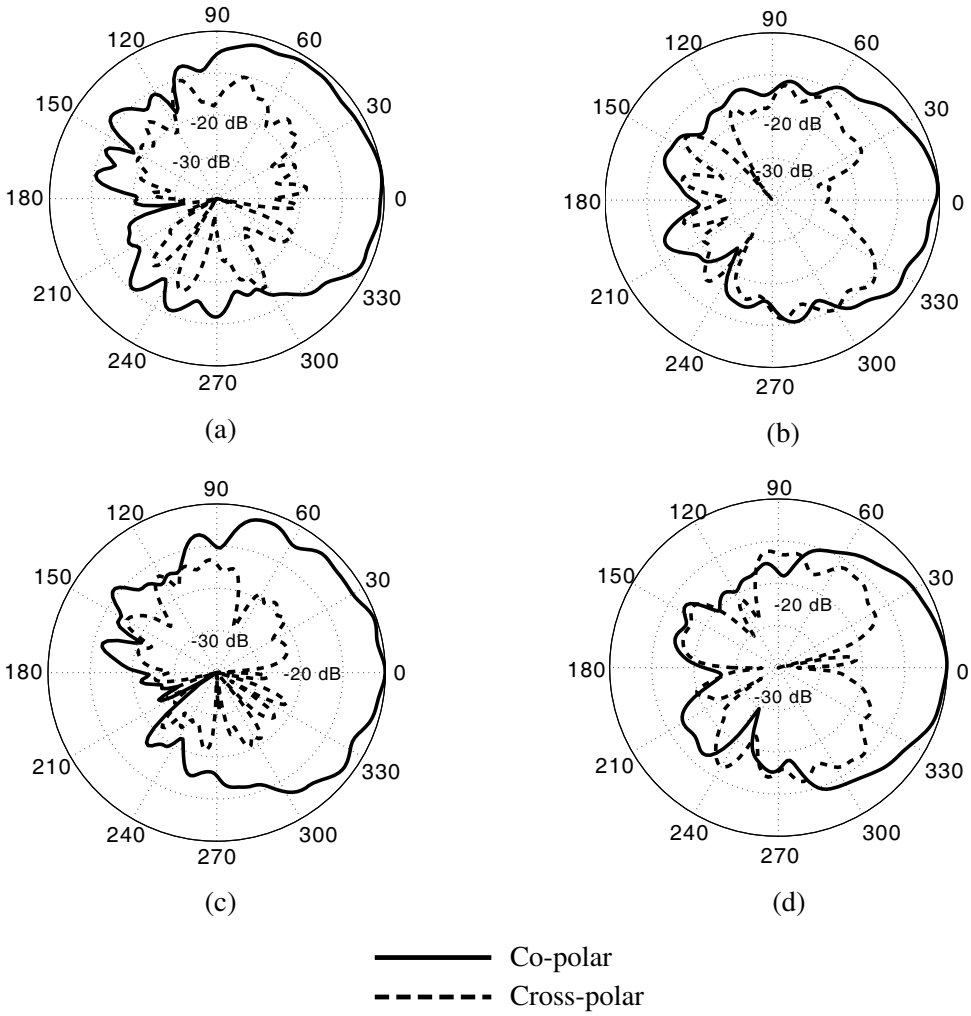

Figure 9. Radiation pattern of patch antenna with and without solar cells under it. (a) E-plane pattern for the patch with solar cells. (b) H-plane pattern for the patch with solar cells. (c) E-plane pattern for the patch without solar cell. (d) H-plane pattern for the patch without solar cell.

corresponding to Figs. 3 and 4 are listed in Table 3. It is again seen that impedance of the antenna with solar cell under it has been affected by the solar cell, and we have to tune the antenna to achieve a better matching. The measured S_{11} data for the antenna with (after being tuned for the impedance matching) and without solar cells are plotted in Fig. 10. It is seen that in the two cases, the antenna resonated at 5 and 4.83 GHz respectively. The normalized radiation pattern is plotted in Fig. 11, and the same conclusion drawn in Section 3.2 stands for this study. The gains of the antenna with and without solar cells were measured to be 2.4 and 5 dB, yielding a difference of 2.6 dB, which is consistent with the results in Section 3.2.

3.4. Effect of the Working Status of the Solar Cells

One of the questions frequently being asked for antennas integrated with solar panels is whether or not the working status of the solar cells affects the antenna. In other words, whether the current in the electrodes of working solar cells affects the antenna. To address this question, we measured S_{11}, radiation pattern, and the gain of the antenna on a solar cell (Fig. 1), when the solar panel was illuminated by an artificial light with varying intensity. We have also measured these parameters by opening, shorting, and connecting different resistive loads to the connector of the solar panel. The tests were repeated for

Table 3. Geometrical parameters of the antenna on plexiglass.

Parameter	Value (mm)	Parameter	Value (mm)
L	19.1	S_i	5.9
W	23.5	W_f	3.8
S_g	1.9	L_f	12.1
h	1.3		

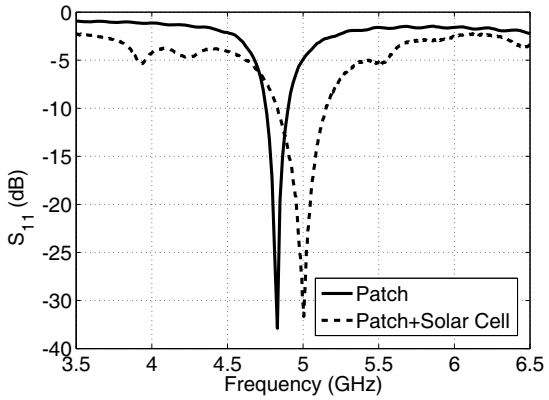

Figure 10. Repetitive Test: Effect of solar cells on the S_{11} parameter of the patch antenna.

both cases where the AF32 and Plexiglass were used as cover glass. From the test results, there was no significant difference observed for the antenna's performance (S_{11}, radiation pattern, gain) at different status of the solar cells. In particular, the decrease due to the solar cell on the antenna's gain remained the same (2–3 dB) regardless of the working status of the solar cells.

3.5. Effect of Solar Panel Geometry

To understand whether the assessment on the gain loss of the antenna due to the solar cell is dependent on the solar panel geometry (i.e. number of solar cells, orientation of solar cells), the following simulative studies have been performed. From the experimental results, we entered the fixtures in Fig. 1 into HFSS by modeling the solar cell as a Ge substrate with added conductivity (σ). Then we adjusted σ until achieving 2.5 dB gain loss of the antenna from the case where there is no solar cell (Fig. 2). After that, the structure is altered into a one-cell solar panel as in Fig. 12 while keeping all the parameters the same except the size of the panel and number of solar cells. It is found that the gain loss on the antenna due to the solar cell is still within 2–3 dB range for an antenna that operates around 4.9 GHz.

In addition, from experiments, the orientation of the solar cells (or the orientation of the antenna relative to the solar cell, such as in Fig. 12(a) and Fig. 12(b)) has shown very small or little effect on the antenna.

3.6. Effect of Air Gap or Adhesive Layer

The results in 3.2 showed that the solar cell shifted the resonant frequency of the antenna upwards, contradictory to the previous results [12]. This is mostly due to the possible air gaps between solar cell and the AF32 cover glass. In Shynu's study [12], the solar cell is a bare cell without cover glass. Therefore, the solar cell may increase the overall effective permittivity of the substrate for the antenna, and accordingly lower the resonant frequency. To verify the effect of the air gap, which is possible in our assembly as solar cell and glass were clipped together, we entered the fixture in Fig. 1 into HFSS, and added an air layer between the solar cell and the glass. The antenna geometry is kept the same as

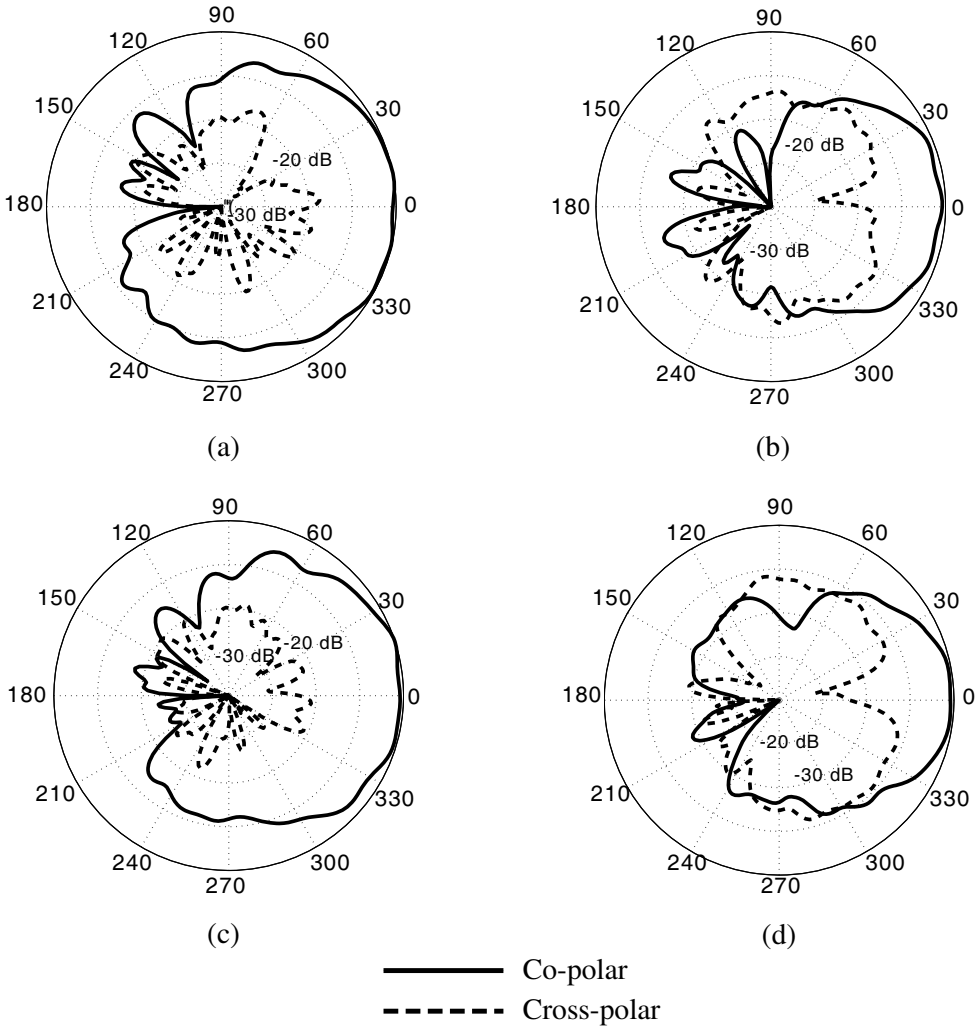

Figure 11. Repetitive Test: Radiation pattern of patch antenna with and without solar cells under it. (a) E-plane pattern for the patch with solar cells. (b) H-plane pattern for the patch with solar cells. (c) E-plane pattern for the patch without solar cell. (d) H-plane pattern for the patch without solar cell.

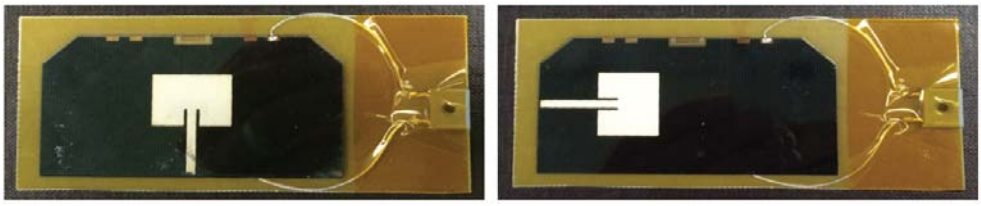

Figure 12. Antenna integrated on a single solar cell. (a) Orientation 1. (b) Orientation 2.

in Table 1 and it resonates at 4.87 GHz when there is no solar cell (Fig. 2). The effect of the air layer is summarized in Table 4, where h_{air} is the thickness of this layer and f_r is the resonant frequency. It is seen that when there is no air gap, the solar cell shifts the f_r downward. When an air layer is present, even if it is very thin such as 50 µm, f_r is shifted to be higher than the case when there is no solar cell.

In space solar cell manufacturing, it is a common practice to use a highly transparent adhesive

layer to bond a solar cell with its cover glass. An example of such adhesive is Dow Corning 93–500 Space Grade Encapsulant 115 Gram (g) Kit [24], which has a dielectric constant of 2.59 at 100 kHz. While recognizing that this ϵ_r may be different at 5 GHz, we used it for study purposes and the results are summarized in Table 4, with $h_{adhesive}$ being the thickness of the adhesive layer. It is seen again that the inclusion of an adhesive material, which is necessary in space application, between cover glass may affect the resonant frequency of the antenna. Most adhesive has lower ϵ_r than the cover glass, and therefore, the solar cell and the adhesive shift the resonant frequency to opposite directions. Depending on the material and thickness of the adhesive, the final resonant frequency of the antenna may not be affected (e.g., when adhesive is between 0.1 mm and 0.15 mm according to Table 4) or shifted slightly up or down from the case when there is no solar cell.

Table 4. Effect of air gap and adhesive layer.

h_{air} (mm)	f_r (GHz)	$h_{adhesive}$ (mm)	f_r (GHz)
0	4.68	0	4.68
0.05	5.02	0.05	4.78
0.1	5.22	0.1	4.83
0.15	5.4	0.15	4.89

4. CONCLUSION

The paper presents a series of detailed experimental studies to quantify the effect of a real-world active space solar cell on a solid patch antenna integrated on it. Test fixtures, with RF ground electrically isolated from the solar cells, were fabricated to study the frequency response, input impedance, radiation pattern, and gain of a patch antenna designed at 4.9 GHz when there is an active solar cell under the antenna. It is found that the solar cell affects the input impedance of the antenna, and more importantly, reduces the gain of the antenna for 2–3 dB. The shape of the radiation pattern and cross-polarization level are not affected by the solar cells. Solar cell alone may shift the resonant frequency of the antenna downward, however, such conclusion claimed by previous study may not be applicable in space applications as it is a common practice that solar cells are bonded with cover glass with an adhesive layer, which normally has a smaller dielectric constant than cover glass. Therefore, the combined affect on the resonant frequency from the solar cell and adhesive may not be dramatically different from when the antenna is designed on the cover glass only. In addition, it is found that the effect of the solar cells on the antenna does not vary for the different working states of the solar cells. In other words, the DC current in the electrodes of the solar cells has little effect on the antenna performance. On the reliability side, three types of repetitive tests were performed. First, five repetitive tests were performed on AF32 cover glass. Next, a Plexiglass substrate was used as the cover glass, and we saw the gain decrease of the antenna due to solar cell was consistent. Finally, the antenna was studied on a single solar cell, and the effect of the solar cell on the antenna remained the same as the prior tests. Although the experiments were performed at 4.9 GHz, it is reasonable to expect a similar result for frequencies around 5.0 GHz, which may be the next frequency of interest for CubeSat community. In summary, it has been shown consistently that one needs to expect a 2–3 dB gain reduction of a patch antenna operating at the vicinity of 5.0 GHz when being integrated on top of a common commercial triple junction solar cell. This will provide an important design consideration and entry to the link-budget for CubeSat missions.

ACKNOWLEDGMENT

We express our gratitude to the National Science Foundation for funding this project (Award 1128622), to Mr. Kelby Davis from the Space Dynamics Laboratory for fabricating the fixtures, and to Dr. John Pratt at Utah State University for proofreading and helpful suggestions.

REFERENCES

1. Vaccaro, S., P. Torres, J. R. Mosig, A. Shah, J. F. Zurcher, A. K. Skrivervik, F. Gardiol, P. de Maagt, and L. Gerlach, "Integrated solar panel antennas," *Electron. Lett.*, Vol. 36, No. 6, 390–391, 2000.
2. Zawadzki, M. and J. Huang, "Integrated RF antenna and solar array for spacecraft application," *IEEE International Conference on Phased Array Systems and Technology*, Dana Point, CA, 2000, 239–242.
3. Wu, T., R. Li and M. M. Tentzeris, "A mechanically stable, low profile, omnidirectional solar-cell integrated antenna for outdoor wireless sensor nodes," *Antennas and Propagation Society International Symposium (APSURSI 2009)*, 14, Charleston, SC, 2009.
4. Shahvirdi, T. and R. Baktur, "A study on the effect of space solar cells on the antennas integrated on top of their cover glass," *Antennas and Propagation Society International Symposium (APSURSI 2014)* , Memphis, TN, 2014, 215–216.
5. Tanaka, M., Y. Suzuki, and K. Araki, "Microstrip antenna with solar cells for microsatellites," *Electron. Lett.*, Vol. 31, No. 1, 56, 1995.
6. Vaccaro, S., J. R. Mosig, and P. de Maagt, "Two advanced solar antenna "SOLANT" designs for satellite and terrestrial communications," *IEEE Trans. Antennas Propag.*, Vol. 51, No. 8, 2028–2034, 2003.
7. Yurduseven, O., D. Smith, and M. Elsdon, "A solar cell stacked multislot quad-band PIFA for GSM, WLAN and WiMAX networks," *IEEE Antennas Wireless Propag. Lett.*, Vol. 23, 285–287, 2013.
8. Mahmoud, M., R. Baktur, and R. Burt, "Fully integrated solar panel slot antennas for small satellites," *Proc. 15th Annual AIAA/USU Conf. on Small Satellites*, Logan, UT, Aug. 2010.
9. Wu, T., R. Li, and M. M. Tentzeris, "A scalable solar antenna for autonomous integrated wireless sensor nodes," *IEEE Antennas Wireless Propag. Lett.*, Vol. 10, 510–513, 2011.
10. Caso, R., A. D'Alessandro, A. Michel, and P. Nepa, "Integration of slot antennas in commercial photovoltaic panels for stand-alone communication systems," *IEEE Trans. Antennas Propag.*, Vol. 61, No. 1, 62–69, 2013.
11. Turpin, T. W. and R. Baktur, "Meshed patch antennas integrated on solar cells," *IEEE Antennas Wireless Propag. Lett.*, Vol. 52, 693–696, 2009.
12. Shynu, S. V., M. J. Roo-Ons, M. J. Ammann, S. J. McCormack, and B. Norton, "Integration of microstrip patch antenna with polycrystalline silicon solar cell," *IEEE Trans. Antennas Propag.*, Vol. 57, No. 12, 3969–3972, 2009.
13. Lim, E. H. and K. W. Leung, "Transparent dielectric resonator antennas for optical applications," *IEEE Trans. Antennas Propag.*, Vol. 58, No. 4, 1054–1059, 2010.
14. Roo-Ons, M. J., S. V. Shynu, M. J. Ammann, S. J. McCormack, and B. Norton, "Transparent patch antenna on a-Si thin-film glass solar module," *Electron. Lett.*, Vol. 47, No. 2, 85–86, 2011.
15. Yurduseven, O., D. Smith, and M. Elsdon, "UWB meshed solar monopole antenna," *Electron. Lett.*, Vol. 49, No. 9, 58–84, 2013.
16. Yasin, T. and R. Baktur, "Circularly polarized meshed patch antenna for small satellite application," *IEEE Antennas Wireless Propag. Lett.*, Vol. 12, 1057–1060, 2013.
17. Dreyer, P., M. Morales-Masis, S. Nicolay, C. Ballif, and J. Perruisseau-Carrier, "Copper and transparent-conductor reflectarray elements on thin-film solar cell panels," *IEEE Trans. Antennas Propag.*, Vol. 62, No. 7, 3813–3818, 2014.
18. Shahvirdi, T. and R. Baktur, "Analysis of the effect of solar cells on the antenna integrated on top of their cover glass," *Antennas and Propagation Society International Symposium (APSURSI 2015)*, 2429–2430, Vancouver, 2015.
19. Henze, N., C. Bendel, J. Kirchhof, and H. Fruchting, "Application of photovoltaic solar cells in planar antenna structures," *Proc. 12th Int. Conf. on Antennas and Propagation*, 731–734, Exeter, U.K., Mar. 2003.

20. Henze, N., M. Weitz, P. Hofmann, C. Bendel, J. Kirchoff, and H. Fruchting, "Investigations on planar antennas with photovoltaic solar cells for mobile communications," *Proc. IEEE Int. Symp. on Personal, Indoor and Mobile Radio Communications*, 622–626, Sep. 2004.
21. Oh, J., K. Lee, T. W. Hughes, S. Forrest, and K. Sarabandi, "Flexible antenna integrated with an epitaxial lift-off solar cell array for flapping-wing robots," *IEEE Trans. Antennas Propag.*, Vol. 62, No. 8, 4356–4361, 2014.
22. [Online]. Available: http://www.emcore.com.
23. [Online]. Available: http://www.schott.com.
24. [Online]. Available: http://www.ellsworth.com.